

Fast library-driven approach for implementation of the voxel spread function technique for correcting magnetic field inhomogeneity artifacts

Jie Wen¹, Feiyan Zeng¹, Dmitriy Yablonskiy², Alexander Sukstansky², Ying Liu¹, Bin

Cai³, Yong Zhang⁴, Weifu Lv¹

1. Radiology, The First Affiliated Hospital of USTC, Division of Life Sciences and Medicine, University of Science and Technology of China, Hefei, Anhui, China, 230001
2. Radiology, Washington University in St. Louis, St. Louis, MO, USA, 63110
3. Radiation Oncology, Washington University in St. Louis, St. Louis, MO, USA, 63110
4. GE Healthcare, Shanghai, China, 201203

Corresponding author:

Jie Wen, PhD

Email: jjewen@ustc.edu.cn

Tel: +86-0551-62283486

Radiology, The First Affiliated Hospital of USTC, Division of Life Sciences and Medicine, University of Science and Technology of China, Hefei, Anhui, China, 230001

Key words: voxel spread function, library, fast calculation, R2*, gradient echo

Word count: 1503

Abstract

Purpose: Previously-developed Voxel Spread Function (VSF) method (Yablonskiy, et al, MRM, 2013;70:1283) provides means to correct artifacts induced by macroscopic magnetic field inhomogeneities in the images obtained by multi-Gradient-Recalled-Echo (mGRE) techniques. The goal of this study is to develop a library-driven approach for fast VSF implementation.

Methods: The VSF approach describes the contribution of the magnetic field inhomogeneity effects on the mGRE signal decay in terms of the F-function calculated from mGRE phase and magnitude images. A pre-calculated library accounting for a variety of background field gradients caused by magnetic field inhomogeneities was used herein to speed up calculation of the F-function and to generate quantitative R2* maps from the mGRE data collected from two healthy volunteers.

Results: As compared with direct calculation of the F-function based on a voxel-wise approach, the new library-driven method substantially reduces computational time from several hours to few minutes, while, at the same time, providing similar accuracy of R2* mapping.

Conclusion: The new procedure proposed in this study provides a fast post-processing algorithm that can be incorporated in the quantitative analysis of mGRE data to account for background field inhomogeneity artifacts, thus can facilitate the applications of mGRE-based quantitative techniques in clinical practices.

1. Introduction

It is well-known that macroscopic B_0 magnetic field inhomogeneities adversely affect quantitative measurements of relaxation parameters obtained with multi-Gradient-Recalled-Echo (mGRE) MRI (1) if not accounted for.

It was demonstrated recently that a voxel spread function (VSF) method of correcting field inhomogeneities (2) incorporated in a quantitative mGRE-based approach (3) provides quantitative information on brain tissue cellular structure (4) as well as its alterations under healthy aging (4) and different neurological diseases (5-8). The VSF method takes advantage of utilizing both magnitude and phase of mGRE data from a single scan, hence it saves acquisition time and avoids misregistration errors. However, a direct implementation of the VSF method requires a large number of voxel-dependent convolutions resulting in long computational time.

In this study, we propose a library-driven approach for fast implementation of the VSF method. Instead of the direct voxel-wise calculation, a pre-calculated library accounting for a variety of background field gradients caused by magnetic field inhomogeneities is used. The library-driven approach substantially reduces the computational time of VSF from hours to a few minutes, and provides similar accuracy compared with the direct calculation. This can facilitate the applications of mGRE-based quantitative techniques in clinical practices.

2. Methods

2.1 Brief Overview of the VSF method

As described in Ref. (8), the image of mGRE-MRI can be expressed as:

$$S_n(TE) = \sum_m \Psi_{nm}(TE) \cdot \sigma_m(TE) \quad [1]$$

where $S_n(TE)$ is the complex images, $\sigma_m(TE)$ is the “ideal” signal from the m^{th} voxel that is free from B_0 -field inhomogeneity artifacts. $\Psi_{nm}(TE)$ is a voxel-dependent convolution kernel, which in the 3D case can be presented as:

$$\Psi_{nm}(TE) = \exp(i\omega_m \cdot TE + i\varphi_0) \cdot \eta_x \cdot \eta_y \cdot \eta_z \quad [2]$$

where the voxel indices n and m are considered as 3D vectors: (n_x, n_y, n_z) and (m_x, m_y, m_z) , ω_m is the frequency shifts. φ_0 is the signal phase shift at $TE=0$, mainly resulted from RF field inhomogeneities. The factors η_j ($j = x, y, z$) have the form:

$$\eta_j = \sum_{q=1}^{N_q} \text{sinc}(q - q_{mj}(TE)) \cdot \exp(2\pi i q (n_j - m_j)) \quad [3]$$

where $q = \{-1/2, -1/2 + 1/N_q, \dots, 1/2 - 1/N_q\}$ is the 1D normalized k -space. For images obtained with the Hanning filter, Eq. [3] should be modified by adding an additional factor $\cos^2(\pi q)$.

The parameters q_{mj} describe phase dispersion across the m^{th} voxel:

$$q_{mj}(TE) = \frac{1}{2\pi} (\mathbf{g}_{mj} \cdot TE + G_{mj}) \quad [4]$$

where \mathbf{g}_m and \mathbf{G}_m are the gradients for the m^{th} voxel calculated from the spatially unwrapped frequency ω and phase φ_0 , respectively. In the 2D case, the factor $\eta_z = \text{sinc}(q_{mz}(TE))$.

Using the similarity approximation,

$$\sigma_m (TE) \Rightarrow \sigma_n (TE) \frac{|S_m (0)|}{|S_n (0)|} \quad [5]$$

Eq. [1] reduces to

$$S_n (TE) = \sigma_n (TE) \cdot F_n (TE) \quad [6]$$

where the F -function, describing the influence of $B0$ field inhomogeneities on images, is given by

$$F_n (TE) = \frac{1}{|S_n (0)|} \sum_m \Psi_{nm} (TE) \cdot |S_m (0)| \quad [7]$$

In practice, the sum in Eq. [7] is taken over several voxels adjacent to a given voxel n . Even for few neighbors included in this sum (see (10)), a large number of voxel-dependent convolutions leads to long computational time. For a typical head scan using mGRE sequence with a matrix size of $256 \times 256 \times 72 \times 10$, the calculation time of the F -function in Matlab using 4 neighbors (in each direction) could take several hours on a computer with typical configurations.

2.2 Library-driven approach

In the voxel-wise direct calculation, the factors η are calculated independently for each voxel. As mentioned above, this procedure usually costs long computational time. In this study, we propose a new way to substantially accelerate the calculation by using a pre-calculated library for η . As shown in Eq. [3], the factors η depend on three parameters: the phase dispersion q_m , neighbor index $(n-m)$, and N_q . When phased-array coils and channel combination methods (4) are used, the parameter q_m depends only on the frequency gradient g_m . In the human brain, the maximum g_m is

well below 1500 rads/voxel. When using an accuracy of 0.1 rads/voxel, a total number of 30,000 points is sufficient to build the library for η . Although η also depends on the number of q -points in the sum in Eq. [3], our simulation shows that as long as using a sufficient large $N_q \geq 256$, the factor η is fairly stable (see **Figure 1**).

Since changing the sign of either q_m or neighbor index $(n-m)$ will result in a complex conjugate of η , one can only use non-negative values of q and non-negative neighbor index $(n-m)$ for calculations. This can further reduce the computational time for library building. This library of η is then used for F -function calculation: for each voxel and its neighbors with particular g_m values, corresponding values of η can be readily found from the library. Importantly, replacing the direct computation by this new library-driven approach substantially reduces the computing time from hours to a few minutes. As long as including sufficiently large N_q and number of neighboring voxels, the library only needs to be built once and can be used for future calculations.

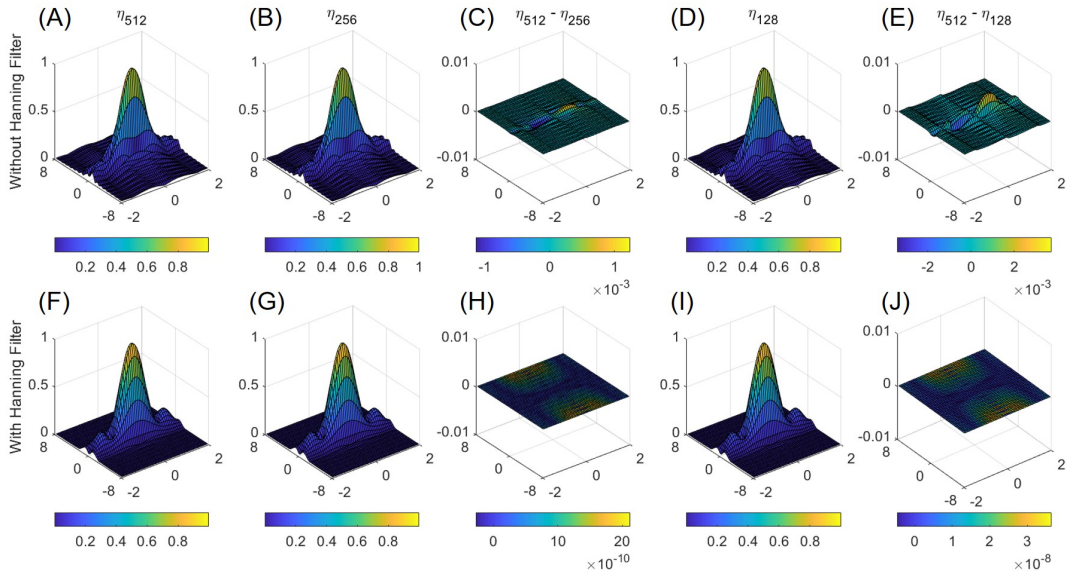


Figure 1 Simulation of η as a function of the distance from a given voxel to the neighboring voxel (-8 to 8) and the parameter $q_m \in (-2, 2)$. A-E: η for the non-filtered

data; F-J: η for the Hanning filtered data. The factor η calculated with $N_q = 512$ (A and F), $N_q = 256$ (B and G) and $N_q = 128$ (D and I) points are shown. The corresponding differences are shown in C, E, H and J. It turns out that when using a sufficient large number of q -points in the sum in Eq. [3] ($N_q \geq 256$), the changes of the values of η are small ($< 1.5 \times 10^{-3}$ for the non-filtered data and $< 2.5 \times 10^{-10}$ for the Hanning filtered data).

2.3 Image acquisition and processing

Images were collected from two healthy volunteers (both are 26 years old female) using a 3T MRI scanner (GE Discovery 750w) equipped with a 12-channel phased-array head coil. All studies were approved by the IRB of The First Affiliated Hospital of USTC. All the participated healthy volunteers have provided written consents.

High resolution datasets with a voxel size of $1 \times 1 \times 2 \text{ mm}^3$ were acquired using a three dimensional (3D) mGRE sequence (ESWAN on GE scanners) with a flip angle of 20° and $TR=50.4 \text{ ms}$. For each acquisition, 10 echoes were collected with first echo time $TE1 = 3.4 \text{ ms}$ and echo spacing $\Delta TE = 3.8 \text{ ms}$. The total acquisition time was around 11 min. The complex images from different channels were combined using a previously introduced method (4,11). The combined mGRE datasets were then used for calculation of the F -function and transverse relaxation rate constant ($R2^*$). The libraries were built for 3 different values of the parameter N_q (512, 256, 128). The F -function was calculated with 4 neighbors for Hanning-filtered data and 16 neighbors for non- filtered data. A maximum value of 1500 rads/voxel and a step of 0.1 rads/voxel were used for the

gradient g_m . All computations were done in Matlab2019a (The MathWorks, Inc., Natick MA, USA) on a computer with standard configurations: 3.2 GHz CPU and 16 GB RAM.

3. Results

Figure 2 shows the comparisons of fitted $R2^*$ maps without and with the F -function. Similarly to (12), the results show that the F -function significantly reduces magnetic field inhomogeneity artifacts on $R2^*$ maps, as indicated by red arrows in **Figure 2**.

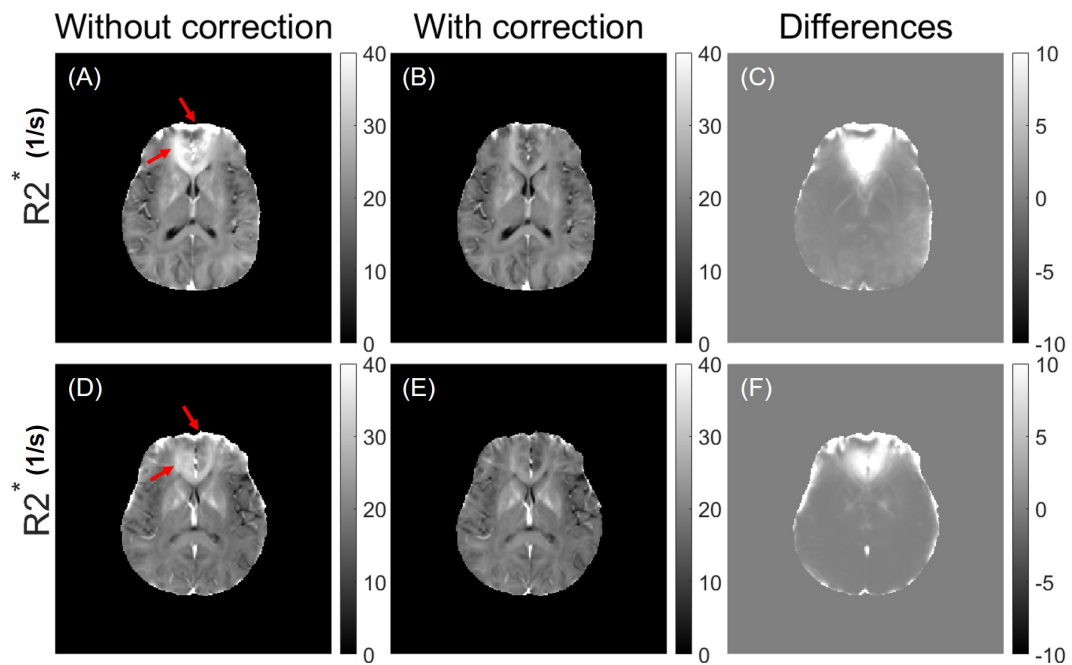


Figure 2 Examples of $R2^*$ maps calculated without (A and D) and with (B and E) F -function and their differences (C and F) for two healthy volunteers (both are 26 years old female). Regions substantially affected by the B_0 field inhomogeneity are indicated by red arrows. The Hanning-filtered data were used for $R2^*$ calculation.

The comparison of the F -functions calculated using direct voxel-wise calculation and library-driven approach are shown in **Figure 3**. The direct calculation of the F -function

required about 5.5 hours on a computer with a 3.2 GHz CPU and 16 GB RAM, while the new method requires only 3 minutes on the same computer. The differences are well below 10^{-4} for the F -function and 10^{-3} for $R2^*$, respectively (panels C, F).

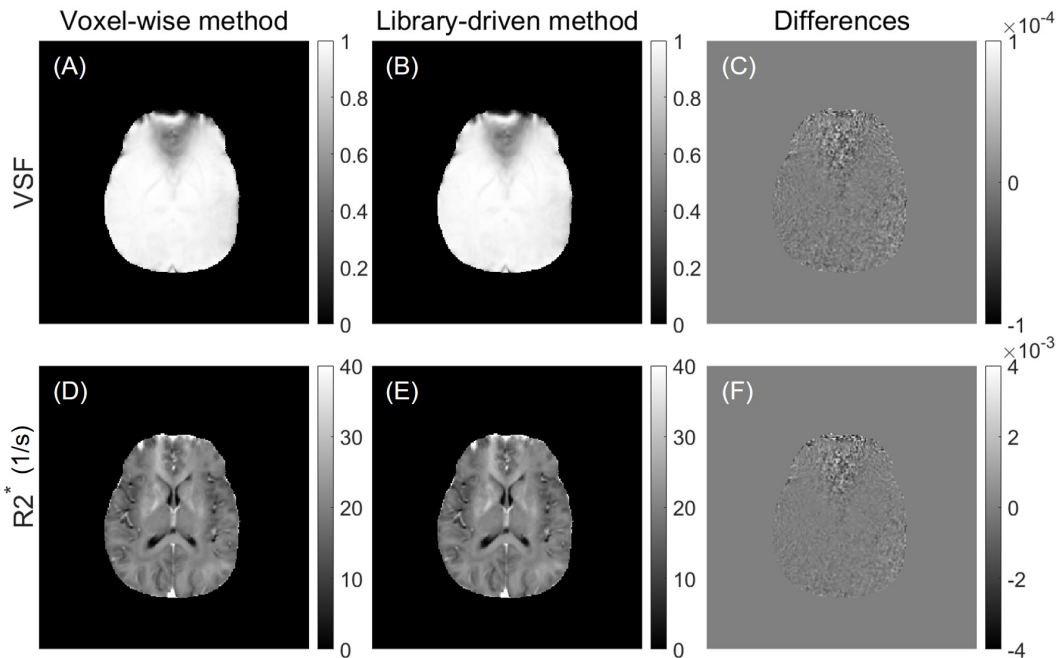


Figure 3 Comparison of the F -function at TE = 37.5 ms (A-C) and $R2^*$ maps (D-F) using voxel-wise method (A and D) and new library-driven method (B and E). The differences are shown in C and F. The Hanning-filtered images were used to calculate the F -function and $R2^*$ maps.

Figure 4 compares $R2^*$ maps calculated using the F -function with different numbers of neighbors included in the sum in Eq. [7]. As demonstrated previously (4), using 4 neighbors (in each direction) is sufficient to get accurate $R2^*$ values from Hanning-filtered data, while for non-filtered data, more neighbors (16 at least) are required.

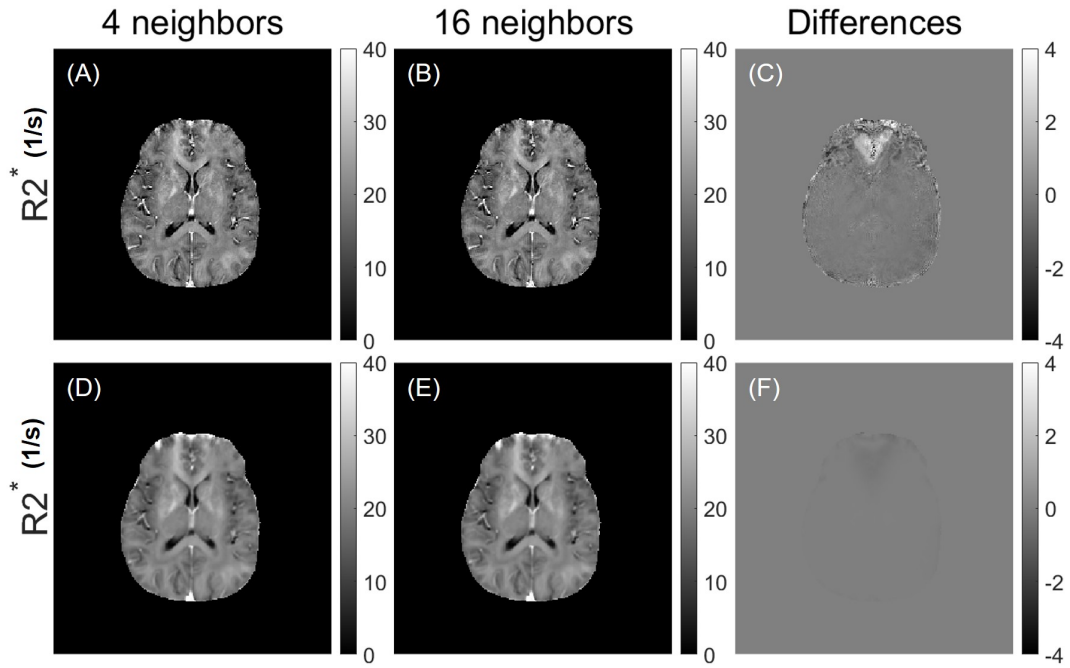


Figure 4 Comparison of $R2^*$ maps calculated using the F -function with different number of neighboring voxels included in the sum in Eq. [7]. Results for non-filtered (A-C) and Hanning-filtered (D-F) data are shown.

$R2^*$ maps calculated using the F -function with different number of q -points N_q are shown in **Figure 5**. Accurate $R2^*$ calculations are guaranteed when sufficient large number of q -points in Eq. [3] ($N_q \geq 256$) are employed, which coincides with the simulation results.

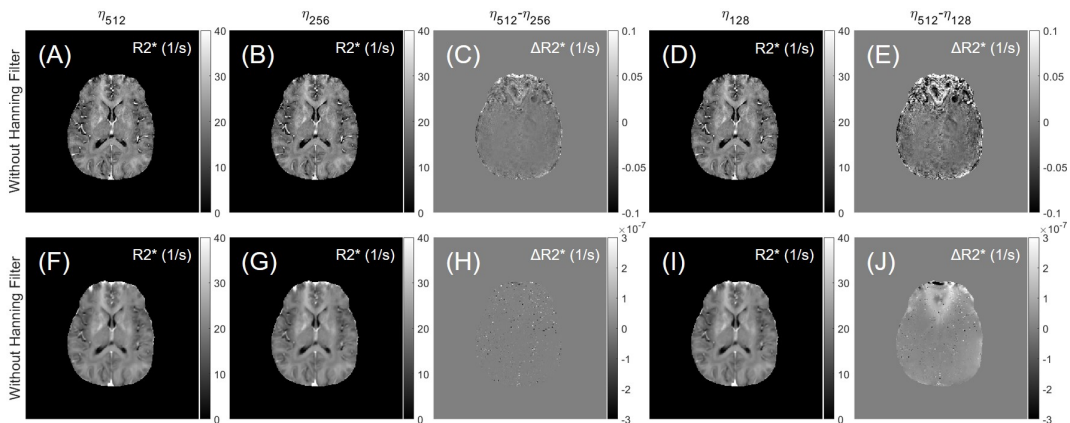


Figure 5 Comparison of $R2^*$ maps calculated using F-function with different number of

q - points N_q (A and F: 512 points; B and G: 256 points; D and I: 128 points). $R2^*$ and differences ($\Delta R2^*$) maps were calculated from non-filtered (A-E) and Hanning-filtered (F-J) data.

4. Discussion and Conclusions

Macroscopic B_0 magnetic field inhomogeneities adversely affect MRI images, especially the ones based on a gradient echo acquisition. They not only lead to image distortions (12), but also degrades quantitative measurements of relaxation parameters (4,13-16) if not accounted for. Numerous methods have been proposed to correct for these adverse effects, including correcting methods during data collection (16-23) and post processing approaches (1,3,24-26). In this paper we focus on the VSF method (27) that allows accounting for the effects of magnetic field inhomogeneities in data obtained with mGRE sequences.

Quantitative parameters that are evaluated using mGRE-based techniques, such as $R2^*$ mapping, are usually suffered from magnetic field inhomogeneity artifacts. These artifacts are extremely severe in those regions that are close to the tissue-air interfaces in sinuses, as shown in **Figure 2**. These artifacts often corrupt the quantitative measurements, thus hinder the clinical application of these quantitative techniques. The VSF method was proposed previously to correct for this effect, however, direct voxel-by-voxel calculations of the F -function requires long computational time. In this study, we presented a library-driven approach for fast VSF implementation. By using a pre-calculated library, the calculation time of the F -function has been reduced from hours

to a few minutes.

We showed through simulations (**Figure 1**) and experiments (**Figure 3**) that by selecting a sufficient number of q -points (N_q) in the sum in Eq. [3] and the number of neighboring voxels included in the sum in Eq. [7] to build the library, the new library-driven method substantially reduces computational time while, at the same time, provides similar accuracy compared with the direct voxel-wise calculation. The reduction of computational time makes it feasible to implement the VSF method with more neighbors included the sum in Eq. [7], which is necessary for non- filtered data.

In conclusion, we presented in this Note a library-driven approach for fast VSF method implementation. The new procedure provides a fast way to correct mGRE-based images for background field inhomogeneity artifacts, thus can facilitate the applications of mGRE-based quantitative techniques in clinical practices.

Acknowledgments

This work was supported by “the Fundamental Research Funds for the Central Universities” WK9110000119.

References

1. Yablonskiy DA. Quantitation of intrinsic magnetic susceptibility-related effects in a tissue matrix. Phantom study. *Magn Reson Med* 1998;39(3):417-428.
2. Fernandez-Seara MA, Wehrli FW. Postprocessing technique to correct for background gradients in image-based R2* measurements. *Magn Reson Med* 2000;44(3):358-366.
3. Hernando D, Vigen KK, Shimakawa A, Reeder SB. R2* mapping in the presence of macroscopic B(0) field variations. *Magn Reson Med* 2012;68(3):830-840.
4. Yablonskiy DA, Sukstanskii AL, Luo J, Wang X. Voxel spread function method

- for correction of magnetic field inhomogeneity effects in quantitative gradient-echo-based MRI. *Magn Reson Med* 2013;70(5):1283-1292.
5. Ulrich X, Yablonskiy DA. Separation of cellular and BOLD contributions to T2* signal relaxation. *Magn Reson Med* 2016;75(2):606-615.
 6. Wen J, Goyal MS, Astafiev SV, Raichle ME, Yablonskiy DA. Genetically defined cellular correlates of the baseline brain MRI signal. *Proc Natl Acad Sci U S A* 2018;115(41):E9727-E9736.
 7. Zhao Y, Wen J, Cross AH, Yablonskiy DA. On the relationship between cellular and hemodynamic properties of the human brain cortex throughout adult lifespan. *Neuroimage* 2016;133:417-429.
 8. Zhao Y, Raichle ME, Wen J, Benzinger TL, Fagan AM, Hassenstab J, Vlassenko AG, Luo J, Cairns NJ, Christensen JJ, Morris JC, Yablonskiy DA. In vivo detection of microstructural correlates of brain pathology in preclinical and early Alzheimer Disease with magnetic resonance imaging. *Neuroimage* 2017;148:296-304.
 9. Xiang B, Wen J, Cross AH, Yablonskiy DA. Single scan quantitative gradient recalled echo MRI for evaluation of tissue damage in lesions and normal appearing gray and white matter in multiple sclerosis. *J Magn Reson Imaging* 2019;49(2):487-498.
 10. Astafiev SV, Wen J, Brody DL, Cross AH, Anokhin AP, Zinn KL, Corbetta M, Yablonskiy DA. A Novel Gradient Echo Plural Contrast Imaging Method Detects Brain Tissue Abnormalities in Patients With TBI Without Evident Anatomical Changes on Clinical MRI: A Pilot Study. *Mil Med* 2019;184(Suppl 1):218-227.
 11. Luo J, Jagadeesan BD, Cross AH, Yablonskiy DA. Gradient echo plural contrast imaging--signal model and derived contrasts: T2*, T1, phase, SWI, T1f, FST2* and T2*-SWI. *Neuroimage* 2012;60(2):1073-1082.
 12. Quirk JD, Sukstanskii AL, Bretthorst GL, Yablonskiy DA. Optimal decay rate constant estimates from phased array data utilizing joint Bayesian analysis. *J Magn Reson* 2009;198(1):49-56.
 13. Ludeke KM, Roschmann P, Tischler R. Susceptibility artefacts in NMR imaging. *Magn Reson Imaging* 1985;3(4):329-343.
 14. Wadghiri YZ, Johnson G, Turnbull DH. Sensitivity and performance time in MRI dephasing artifact reduction methods. *Magn Reson Med* 2001;45(3):470-476.
 15. Merboldt KD, Finsterbusch J, Frahm J. Reducing inhomogeneity artifacts in functional MRI of human brain activation-thin sections vs gradient compensation. *J Magn Reson* 2000;145(2):184-191.
 16. Hwang D, Kim D-H, Du YP. In vivo multi-slice mapping of myelin water content using T2* decay. *NeuroImage* 2010;52(1):198-204.
 17. Frahm J, Merboldt KD, Hanicke W. Direct FLASH MR imaging of magnetic field inhomogeneities by gradient compensation. *Magn Reson Med* 1988;6(4):474-480.
 18. Du YP, Chu R, Hwang D, Brown MS, Kleinschmidt-DeMasters BK, Singel D, Simon JH. Fast multislice mapping of the myelin water fraction using multicompartement analysis of T2* decay at 3T: a preliminary postmortem study. *Magn Reson Med* 2007;58(5):865-870.

19. Haacke EM, Tkach JA, Parrish TB. Reduction of T2* dephasing in gradient field-echo imaging. *Radiology* 1989;170(2):457-462.
20. Cho ZH, Ro YM. Reduction of susceptibility artifact in gradient-echo imaging. *Magn Reson Med* 1992;23(1):193-200.
21. Yang QX, Williams GD, Demeure RJ, Mosher TJ, Smith MB. Removal of local field gradient artifacts in T2*-weighted images at high fields by gradient-echo slice excitation profile imaging. *Magn Reson Med* 1998;39(3):402-409.
22. Wild JM, Martin WR, Allen PS. Multiple gradient echo sequence optimized for rapid, single-scan mapping of R2* at high B0. *Magn Reson Med* 2002;48(5):867-876.
23. Yang QX, Wang J, Smith MB, Meadowcroft M, Sun X, Eslinger PJ, Golay X. Reduction of magnetic field inhomogeneity artifacts in echo planar imaging with SENSE and GESEPI at high field. *Magn Reson Med* 2004;52(6):1418-1423.
24. Truong TK, Chakeres DW, Scharre DW, Beversdorf DQ, Schmalbrock P. Blipped multi gradient-echo slice excitation profile imaging (bmGESEPI) for fast T2* measurements with macroscopic B0 inhomogeneity compensation. *Magn Reson Med* 2006;55(6):1390-1395.
25. Baudrexel S, Volz S, Preibisch C, Klein JC, Steinmetz H, Hilker R, Deichmann R. Rapid single-scan T2*-mapping using exponential excitation pulses and image-based correction for linear background gradients. *Magn Reson Med* 2009;62(1):263-268.
26. Bashir A, Yablonskiy DA. Natural linewidth chemical shift imaging (NL-CSI). *Magn Reson Med* 2006;56(1):7-18.
27. Yang X, Sammet S, Schmalbrock P, Knopp MV. Postprocessing correction for distortions in T2* decay caused by quadratic cross-slice B0 inhomogeneity. *Magn Reson Med* 2010;63(5):1258-1268.